Centroid regression using CNN-based Image Processing Algorithm with application to a binary asteroid system

Aurelio Kaluthantrige
Department of Mechanical and Aerospace Engineering
University of Strathclyde
Glasgow, Scotland, United Kingdom
mewantha.kaluthantrige-don@strath.ac.uk

Jinglang Feng
Department of Mechanical and Aerospace Engineering
University of Strathclyde
Glasgow, Scotland, United Kingdom
jinglang.feng@strath.ac.uk

Jesus Gíl-Fernández
ESA/ESTEC
Noordwijk, The Netherlands
Jesus.Gil.Fernandez@esa.int

Andrea Pellacani
GMV Aerospace and Defence
Madrid, Spain
apellacani@gmv.com

***Abstract*—Autonomous Optical Navigation is essential for the proximity operations of space missions to asteroids that usually have irregular gravity fields. One core component of this navigation strategy is the Image Processing (IP) algorithm that extracts optical observables from images captured by the spacecraft's on-board camera. Among these observables, the centroid of the asteroid is important to determine the position between the spacecraft and the body, which is the focus of this research.**
However, the performance of standard IP algorithms is affected and constrained by the features of the images, such as the shape of the asteroid, the illumination conditions and the presence of additional bodies, therefore, the quality of the extracted optical observables is influenced.
To address the latter two challenges, this paper develops a Convolutional Neural Networks (CNN)-based IP algorithm and applies it to the Early Characterization Phase (ECP) of the European Space Agency's HERA mission with the target body of binary asteroid Didymos.
This algorithm is capable of estimating the centroid of the primary body successfully with high accuracy and without being affected by the presence of the secondary body or the illumination in the input images. In addition, it can also estimate the centroid of the secondary body when the two bodies are in the same image, which increases the robustness of the overall navigation strategy.

***Index Terms*—Centroiding technique, image processing, phase angle, Convolutional Neural Networks, asteroid exploration**

I. Introduction

The Asteroid Impact Deflection Assessment (AIDA) is an international collaboration between the National Aeronautics and Space Administration (NASA) and the European Space Agency (ESA), with the primary objective of investigating a binary asteroid system and to demonstrate its deflection by kinetic impact. The NASA contribution to this mission is the Double Asteroid Redirection Test (DART), a kinetic impactor launched on the 24th of November 2021 that will perform the deflection in September 2022 [1]. ESA's segment of the AIDA mission is represented by HERA, whose objectives are to research on the properties of the binary asteroid system, to observe the results of DART's impact and to assess the feasibility of the deflection technique [2]. The target of this mission is the near-Earth asteroid (NEA) (65803) Didymos and its moon Dimorphos. Table I illustrates relevant properties of Didymos and Dimorphos. The spin axis of both bodies is orthogonal to the binary's orbital plane. Dimorphos is tidally locked with Didymos, i.e. its rotation period is equal to its revolution period around the primary [3].

TABLE I
Didymos' system properties [3]

Parameter	Didymos	Dimorphos
Gravitational parameter $[km^3/s^2]$	$3.5225 \cdot 10^{-8}$	$2 \cdot 10^{-10}$
Diameter $[m]$	780	164
Rotation period $[hours]$	2.26	11.92
Obliquity of the binary orbit with Ecliptic	$169.2°$	$169.2°$

The proximity operations of HERA consist of different phases that depend on the mission objectives. The focus of this work is the Early Characterization Phase, with the spacecraft at a distance of around 30 km from the target with the objective of conducting physical and dynamical characterizations of Didymos [4].
Observing a binary asteroid system from such a short distance is unprecedented. A vision based Guidance, Navigation and Control (GNC) system is designed to improve the mission autonomy. This system comprises an on-board camera

European Space Agency.

This is a peer reviewed, accepted author manuscript of the following conference paper: Kaluthantrige, A., Feng, J., Gil-Fernández, J., & Pellacani, A. (2022). Centroid regression using CNN-based image processing algorithm with application to a binary asteroid system. In 2022 IEEE World Congress On Computational Intelligence IEEE.

taking images of the asteroid, an IP algorithm that extracts information from these images, and a navigation filter that is able to process the visual data to estimate the spacecraft position, velocity and attitude with respect to the binary system. The camera used for the vision based navigation system is the Asteroid Framing Camera (AFC). For the ECP, the navigation strategy is centroid-based, meaning that the IP algorithm is designed to extract the Center of Mass (COM) of the primary body, thus estimating the Line Of Sight (LOS) of the spacecraft, with the purpose of enabling autonomous attitude navigation [5]. Nevertheless, standard IP algorithms' performances are highly depending on the intrinsic properties of the captured images. External factors such as the Signal-to-Noise ratio, illumination conditions and the presence of other bodies in the image can damage the performance of the IP algorithm [6].

This work aims to address the challenges related to the illumination of the asteroid and the presence of Dimorphos in the images. In particular, we develop a CNN-based image processing algorithm that estimates the centroid of the primary without being affected by these two factors. Recent years have seen an increase of the implementation of CNNs in space image processing. One of the main advantages of CNNs with respect to standard IP algorithms is the robustness over disturbances and adverse characteristics of the images [7]. Most of the CNNs process the input image with a network typically consisting of a series of high-to-low resolution subnetworks. This process reduces the input's resolution, which is then recovered through a low-to-high process. With this procedure, extracted visual data have low spatial precision and accuracy that are important aspects for an autonomous attitude navigation system. Therefore, this works adopts the High-Resolution Network (HRNet) architecture to maintain a high-resolution representation through the whole network [8]. This process leads to a features extraction with superior spatial precision and higher accuracy.

For the application to the HERA mission, the HRNet-based algorithm is demonstrated to estimate the centroid of the primary without the dependence on the position of the Sun and the presence of the secondary body in the images. Moreover, the algorithm also manages to measure the centroid of the secondary body, which is a unique contribution to the robustness of the navigation strategy for the ECP phase of HERA.

This paper is structured as follows. Section II reviews the state of the art for centroiding techniques. Then, Section III describes the framework of our methodology. Next, Section IV performs the numerical simulations and analyze the results obtained. Finally, Section V concludes this research and recommends future research directions.

II. Related models

In this Section, current IP algorithms that estimate the position of the centroid of asteroids are reviewed.

Methods that rely on the calculation of the Center of Brightness (COB), that is the centroid of the image when each pixel is weighted by its intensity, have been proposed. An offset depending on the position of the Sun is then applied to determine the COM of the asteroid. Nevertheless, when the lighting circumstances are inadequate, these methods become inaccurate [9]. Data-driven scattering laws have been implemented to solve the dependency of the accuracy on the position of the Sun [10].

Centroid Apparent Diameter (CAD), ellipse and limb fitting techniques rely on the a priori knowledge of the apparent size and shape of the asteroid. Moreover, they require that the shape of the model is regular [11, 12].

The current IP algorithm implemented by HERA for the centroiding problem resolution is the Maximum Correlation with a Lambertian Sphere (MCLS). This algorithm estimates the size of the sphere with Lambertian reflectance that maximises the normalized correlation with the binarized image of the asteroid. Hence, the bright pixels of the image play a major role in this IP technique, thus making it highly depending on the position of the Sun [5].

III. Approach

In this Section, the methodology of this research is described. The methodology consists of three main unites: the reference trajectory of HERA, the generation of the images and the implementation of the HRNet-based centroiding algorithm.

A. Reference trajectory

The reference trajectory considered in this work is the ECP trajectory of HERA provided by ESA. The ECP is aimed to achieve the initial physical and dynamical characterization of the binary system. During this phase, the only navigation instrument available is the AFC camera and it is desired that both the primary and the secondary bodies lie within its Field Of View (FOV). The total duration of the ECP is 6 weeks and the position of HERA is kept at around $20 - 30\ km$ with respect to the primary [4].

Fig. 1 represents the ECP trajectory, together with the orbit of Dimorphos and the position of the Sun, the latter being scaled down in the illustration. The adopted reference frame is the Target Body Equatorial Inertial (TBEqI), with the origin located on the primary, the X-axis pointing towards the vernal equinox, the Z-axis the spin axis of the primary and the Y-axis completing the right-handed frame. Therefore, the XY plane of the TBEqI is coplanar to the equatorial plane of Didymos in which Dimorphos' orbit is located. The relative motion of the Sun around Didymos is retrograde as the orbit obliquity of the binary system with respect to the ecliptic plane (shown in Table I) is higher than 90 degrees. The position of the Sun has been calculated using the Jet Propulsion Laboratory (JPL) Small Body Database [13]. The initial epoch and the final epoch of the ECP are respectively $t_{in} = 9012$ days and $t_{fin} = 9026$ days both in the Modified Julian Date 2000.

The ECP trajectory consists of 4 arcs, and it has been generated considering only the point mass gravitational attraction of both Didymos and Dimorphos and the orbital manoeuvres performed at the joint of two arcs. In order to fulfil the operational and safety constraints as well as the distances defined in the mission analysis, a duration of 3 days has been baselined for the 2^{nd} and 4^{th} arcs and 4 days for the 1^{st} and 3^{rd} arcs [4].

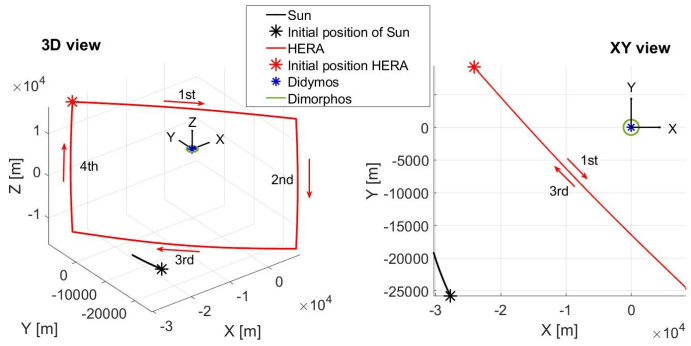

Fig. 1. ECP Trajectory

The XY view in Fig. 1 shows that the ECP trajectory lies between the Sun and Didymos, meaning that HERA is always seeing the day side of the asteroid i.e. when the phase angle γ (Sun-asteroid-HERA angle) is lower than 90 degrees. The nominal operations of the ECP take place only in the day side of Didymos to ensure the validation of AFC images for the centroiding navigation [4]. Fig. 2 shows the value of γ for the reference trajectory. It can be seen that γ reaches its maximum of 77.53 degrees at $t = 9016$ days (end of the 1^{st} arc) and its minimum of 44.38 degrees at $t = 9021$ days (end of 3^{rd} arc).

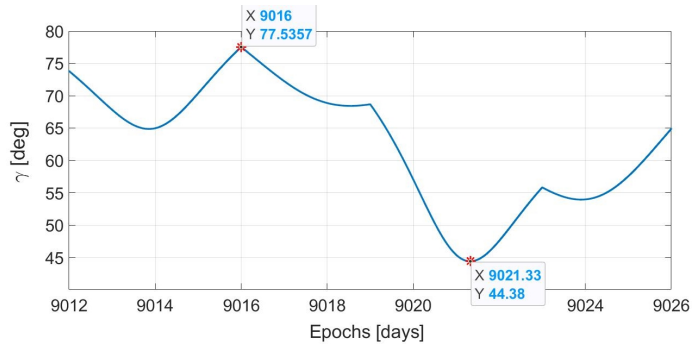

Fig. 2. Phase angle

B. Datasets

The datasets of synthetic images are generated using the software Planet and Asteroid Natural scene Generation Utility (PANGU). This software is a simulation tool that models planet and asteroids surfaces and provides high resolution realistic images at high frame rates. PANGU is being employed widely by ESA to support the verification and validation of vision-based navigation systems.

The models of Didymos and Dimorphos have been provided by GMV Aerospace and Defence. The model of Itokawa, the target asteroid of Hayabusa mission, is scaled down and used as the model for Dimorphos. The software generates the images detected by the camera on the PANGU viewer, a planar reference system with the origin located on the top left corner of the plane, the horizontal axis (referred to as i-direction) and vertical axis (referred to as j-direction) pointing respectively rightward and downward (as shown in Fig. 3), and the unit of measure being pixels.

In order to visualize the binary system of asteroids on PANGU, the flight file system has been operated. These files control the PANGU viewer and generate images taken at different epochs [14]. At each point of the trajectory, the position of the Sun (range, Azimuth and Elevation) and the positions and the orientations (quaternions) of Didymos, Dimorphos and the AFC camera (joined with HERA) have been calculated in the TBEqI and input into the flight file, which regulates the image of the PANGU viewer. The latter has been configured with the parameters of the AFC camera, shown in Table II [15].

TABLE II
AFC PARAMETERS [15]

FOV	Focal Length	Aperture	Image size
5.5°	10.6 cm	2.5 cm	1024 × 1024 $pixels$

During asteroid imaging, the AFC has its boresight pointing towards the asteroid and the vertical axis of the camera is perpendicular to the direction of the Sun with respect to the spacecraft. According to PANGU's conventions, the boresight, the vertical axis and the horizontal axis of the camera are respectively the Z-axis, the Y-axis and the X-axis of the camera reference frame [4, 14]. As a result, the position vector of the Sun with respect to HERA is always coplanar to the XZ plane of the camera frame. Therefore, the images generated on the PANGU viewer always represent the binary system illuminated from the right side. Fig. 3 shows the PANGU viewer for four sample images captured at different points of the four arcs of the ECP trajectory.

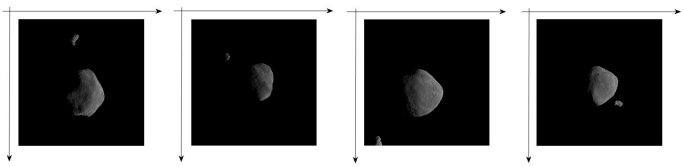

Fig. 3. Sample images captured during the 1st, 2nd, 3rd and 4th arc of the ECP

When the spacecraft is pointing perfectly towards the primary or the secondary, the latter is displayed at the middle of the PANGU viewer. The models of Didymos and Dimorphos implemented in PANGU, in these conditions, have the central pixel, with coordinates $(i, j) = (512, 512)$ pixels, representing the Geometrical Center (GC) of the target body, that is

the arithmetic mean position of all the points of the image belonging to the body.

Because of their quasi-spherical and ellipsoidal shapes, the COMs of the primary and the secondary are very close to their GCs. Since the datasets of images used in this work are all generated with PANGU, the GC of the asteroid will represent its centroid.

Applying a CNN algorithm to a set of images generated when the camera's boresight is pointing perfectly towards the asteroid would result in an issue of label variability as the GC would always have the same value, that is $(i, j) = (512, 512)$ pixels. To overcome this issue an error represented by spherical coordinates using two angles α and β is introduced at each point of the trajectory in the boresight direction of the camera reference system, as shown in Fig. 4, so that the generated image is shifted from its central position.

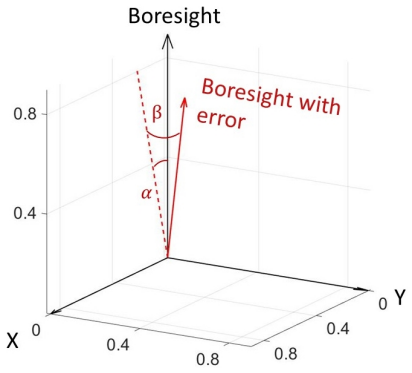

Fig. 4. Camera pointing

Random values within an interval of $[-0.5, 0.5]$ degrees are used for the two angles at each epoch, considering a threshold value driven by the 5.5 degrees FOV of the AFC and the requirement of displaying Dimorphos within the PANGU viewer. The orientation of the boresight with error has been used for the generation of the dataset of images in PANGU.

By calculating the relationship between the angular error and the shift in pixels of the image from the central position, the GCs of both bodies can be calculated, as shown in the example of Fig. 5.

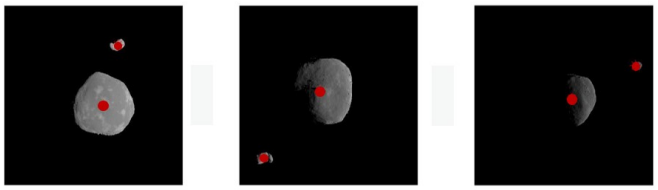

Fig. 5. Sample images generated during the 2nd, the 3rd and 4th arc of the ECP with centroid measurements of Didymos and Dimorphos

C. Implementation of the HRNet

The HRNet architecture is shown in Fig. 6. The network maintains the high resolution representations of the input images by connecting multiple subnetworks in parallel. The first stage is a high-resolution subnetwork. New stages are formed from the gradual addition of high-to-low subnetworks. To maintain the high-resolution representation, repeated multiscale fusions are performed using low-resolution representation of the same depth and similar level. The last high-resolution representation is then used for the regression of the desired visual data (keypoint), in this work being the centroids of Didymos and Dimorphos [8].

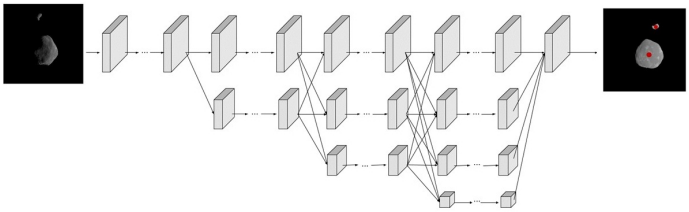

Fig. 6. HRNet architecture

Each input image of the HRNet is coupled with the two corresponding centroids. The latter represent the Ground Truth (GT) keypoints and are used to supervise the training of the HRNet to regress the centroid locations of the testing dataset. In this work, the pose-hrnet-w32 has been used, where 32 represent the widths of the high-resolution subnetwork in the last three stages. The Adam optimizer is used with a cosine decaying learning rate with initial value of 10^{-3} and decaying factor of 0.1. The total parameters involved in the training process are $28,535,618$.

The input database consists of 10083 (61.54%) images for training, 1266 (7.73%) for validation and 5031 (30.73%) for testing obtained by sampling the trajectory respectively every 100, 800 and 200 seconds and discarding the images where Dimorphos is outside of the camera frame or behind the primary. The network is trained for 210 epochs. Fig. 7 shows a mosaic of keypoint detection results on a subset of the training dataset.

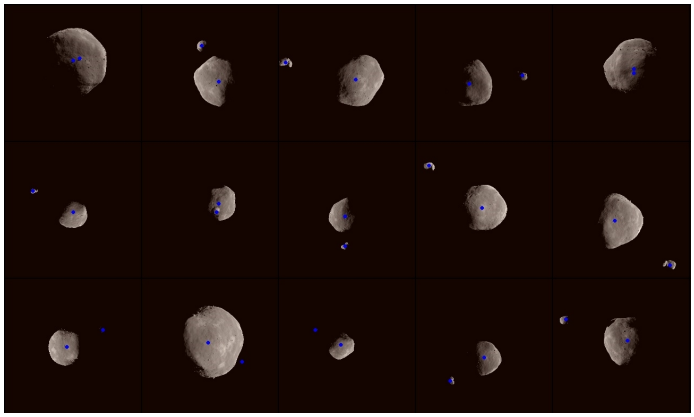

Fig. 7. Sample keypoint detection results during training

IV. Experiments

In this section, the results of the HRNet-based IP algorithm over the database representative of the ECP trajectory of

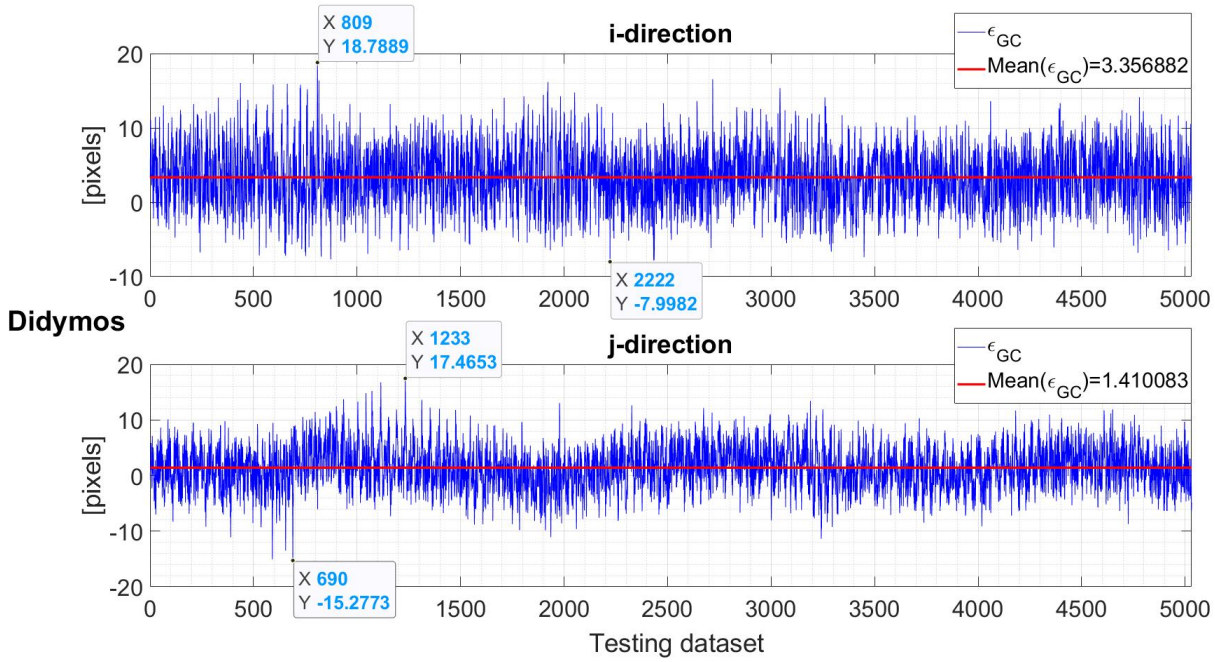

Fig. 8. ε_{GC} for Didymos

the HERA mission are presented. Firstly, the results of the centroiding algorihtm of Didymos are analyzed, by examining the influence of the phase angle and the disturbances due to the appearance of Dimorphos. Secondly, the results of the centroiding algorithm of Dimorphos are presented, examining the particular case of eclipses.

The metrics to evaluate the performances are defined as follows:

$$\varepsilon_{GC} = GC_{GT} - GC_{pred} \tag{1}$$

$$RMSE = \sqrt{\frac{\sum_{i=1}^{N}((GC_{GT}^{i} - GC_{pred}^{i})^2)}{N}} \tag{2}$$

where ε_{GC} represents the real value of the error in pixels between the ground truth GC and the predicted GC, and $RMSE$ is the Root Mean Squared Error (RMSE) in pixels between the same quantities. Both metrics are evaluated for each direction of the PANGU viewer.

To evaluate the accuracy of the developed algorithm, the $RMSE$ values for the i- and j-directions obtained by the MCLS IP algorithm developed by GMV Aerospace and Defence for the HERA mission are given as a reference: $RMSE_i^{GMV} = 5.987$ pixels and $RMSE_j^{GMV} = 4.915$ pixels. These results are obtained by applying the algorithm over a set of 243 images generated during the ECP.

A. Didymos

1) Accuracy: Fig. 8 represents the ε_{GC} for the centroiding of Didymos for both i and j-directions of the PANGU viewer reference frame, for the testing dataset of 5031 images. It can be seen that the error related to Didymos is oscillating around 3.35 pixels in the i-direction with a maximum and a minimum values of 18.78 and -7.9 pixels and around 1.41 pixels in the j-direction with a maximum and a minimum values of 17.46 and -15.27 pixels, respectively. The $RMSE$ values are: $RMSE_i = 5.26$ pixels and $RMSE_j = 4.27$ pixels, which are lower than the ones obtained by the MCLS IP algorithm. Therefore, the HRNet-based IP algorithm is able to estimate the centroid of the primary with higher accuracy.

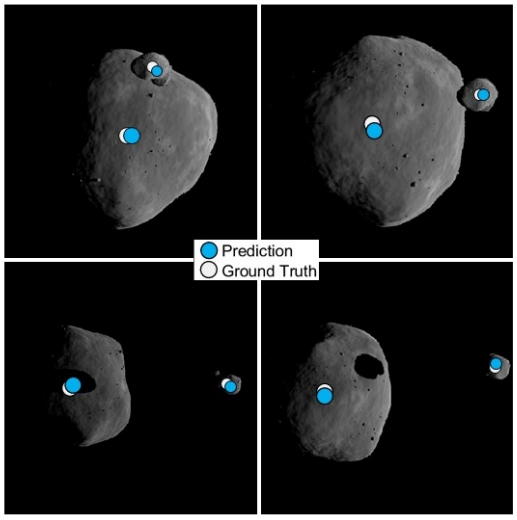

Fig. 9. Centroiding results for images with disturbances due to the presence of Dimorphos

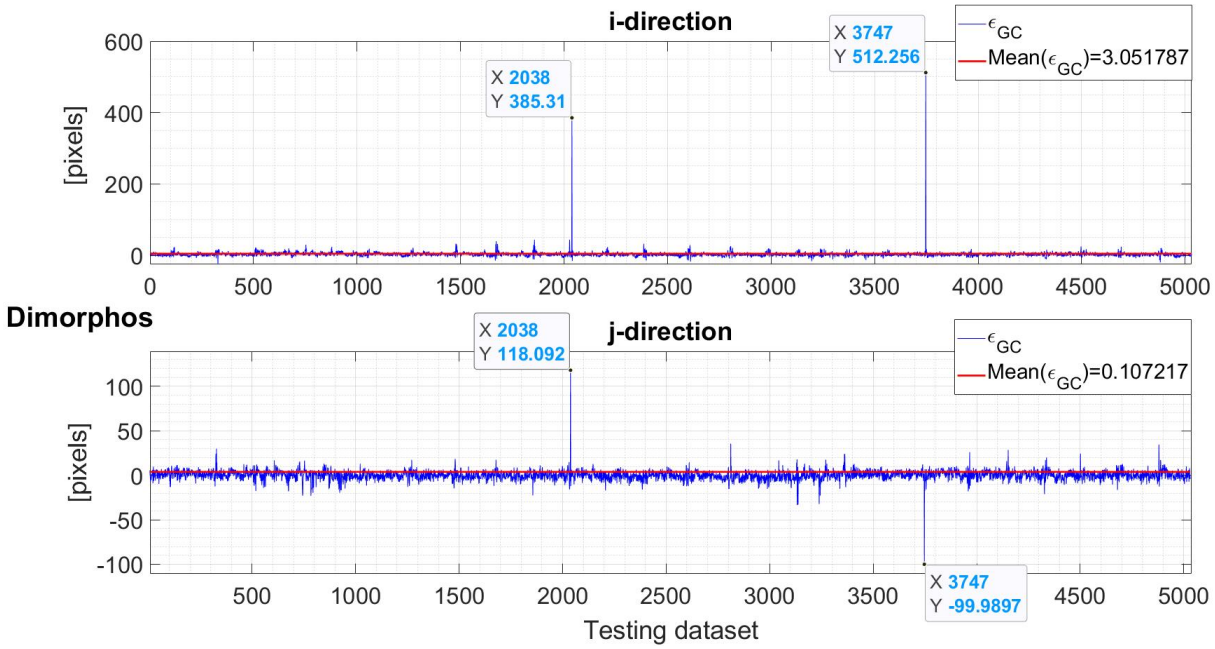

Fig. 10. ε_{GC} for Dimorphos

2) Phase angle: As mentioned in Section III-B, the binary system is always illuminated from the right side in the images. Hence, the influence of the Sun phase angle can be inferred by the results on the i-direction. The systematic error of 3.35 pixels is negligible considering that is lower than the peak-to-peak amplitude (26.68 pixels) of the error itself. Therefore, the developed centroiding algorithm is not affected by the illumination conditions of the asteroid.

3) Dimorphos' disturbance: The subset of images with the projection of the secondary on the surface of Didymos are 193 out of the 5031 of the testing dataset. The RMSE values of the developed centroiding algorithm for these images are: $RMSE_i = 5.88$ pixels and $RMSE_j = 4.50$ pixels. The difference of these values from the ones presented in Section IV-A1 is negligible, hence the performance of the developed algorithm is not affected by this disturbance.
When Dimorphos is located between the Sun and Didymos, its shadow is projected on the surface of the primary. 537 out of the 5031 images of the testing dataset present this condition. For this subset, the values of the RMSE are $RMSE_i = 5.64$ pixels and $RMSE_j = 4.59$ pixels. Therefore, even the shadow of Dimorphos is a negligible disturbance for the performances of the centroiding algorithm. Fig. 9 shows 4 examples of these two disturbances analyzed in this Section.

B. Dimorphos

1) Accuracy: Fig. 10 illustrates the centroiding results of Dimorphos for the i- and j-directions of the PANGU viewer for the 5031 images of the testing dataset. The average value of the error is 3.05 pixels for the i-direction and 0.107 pixels for the j-direction. The RMSE values are $RMSE_i = 10.71$ pixels and $RMSE_j = 5.48$ pixels, which are higher than the ones obtained for the primary body. This lower accuracy is explained by the fact that the shape of the PANGU model of Dimorphos, represented by a scaled down model of Itokawa, is irregular, which is more difficult for the IP algorithm to estimate its GC.

2) Dimorphos in eclipse: There are a total of 593 images of the testing dataset that represent Dimorphos in partial or total eclipse because of the primary's shadow. The centroiding algorithm is still capable of providing an estimation of the centroid as in this subset the secondary's boundary is visible even in total eclipse conditions, as shown in Fig. 11 (the boundary illumination has been enhanced in the figure for illustration purposes). The RMSE values for this subset of

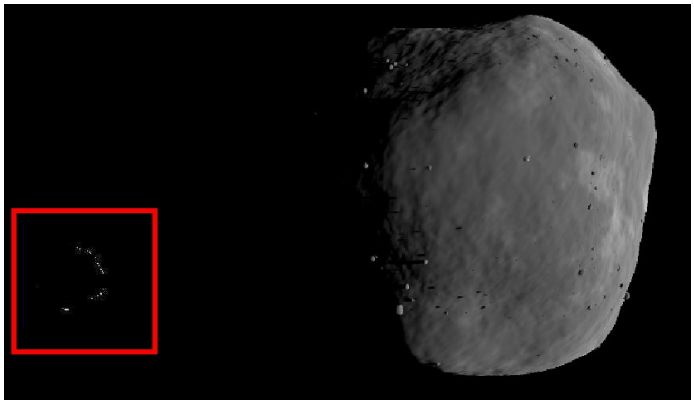

Fig. 11. Illuminated boundary of Dimorphos when eclipse occurs

images are $RMSE_i = 28.39$ pixels and $RMSE_j = 10.43$ pixels. Fig. 12 shows the results of two images representing the partial and the total eclipse of Dimorphos.

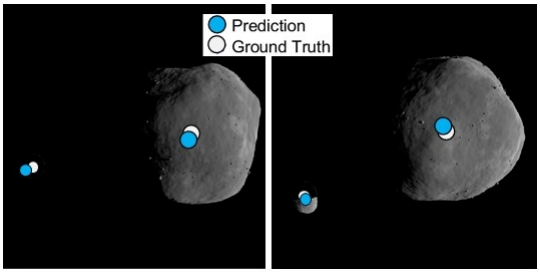

Fig. 12. Dimorphos' centroiding results in partial and total eclipse

It can be seen from Fig. 10 that the IP algorithm fails for image 2038 and 3747 of the testing dataset, as the boundary of Dimorphos is not illuminated enough for the HRNet to determine the centroid position.

V. Conclusions

This paper develops a CNN-based IP algorithm solving the centroiding problem of a binary asteroid system. The ECP proximity operation of HERA mission to Didymos system has been studied as case scenario. The main objective of the developed methodology is to tackle the challenges represented by adverse illumination conditions of the target and by the disturbances caused by the presence of the secondary. Moreover, the algorithm aims to estimate the centroid of the secondary body, increasing the robustness of the next phases of the mission. The database of images has been generated using the software PANGU. The chosen CNN architecture is the HRNet, being the state of the art in keypoint detection, and being already exploited for spaceborn applications.

The results show that the HRNet-based IP algorithm is able to estimate the centroid of the primary with higher accuracy than the MCLS IP algorithm. In particular the method is robust to the presence of Dimorphos and its shadow projected on the surface of the primary, and it exhibits no dependency on the Sun phase angle. If higher accuracy is required, the training database can be augmented using additional images generated from different trajectories around the target.

Moreover, the algorithm estimates with high accuracy the position of the centroid of the secondary body, even in partial and total eclipse conditions, which is a unique contribution of this work.

Future work would go into the direction of other utilizations for the HRNet-based IP algorithm. For instance, additional estimated outputs that are useful for the navigation algorithm of the GNC system during the proximity operations with the asteroid are the range from Didymos and the Sun phase angle.

Acknowledgements

This study is co-funded and supported by the European Space Agency under the Open Space Innovation Platform and supported by the GMV Defence and Space. The authors would like to thank Florin-Adrian Stancu for the contribution with the provided model of Didymos in PANGU. The authors would also like to acknowledge the support of the entire Aerospace Centre of Excellence of University of Strathclyde.

References

[1] P. Michel, A. F. Cheng, and M. Küppers, "Asteroid Impact and Deflection Assessment (AIDA) mission: science investigation of a binary system and mitigation test," in European Planetary Science Congress 2015, held 27 September-2 October, 2015 in Nantes, France, Online at http://meetingorganizer. copernicus. org/EPSC2015, id. EPSC2015-123, 2015, vol. 10, p. 123, [Online]. Available: http://meetingorganizer.copernicus.org/EPSC2015/EPSC2015-123.pdf.

[2] P. Michel, M. Küppers, and I. Carnelli, "The Hera mission: European component of the ESA-NASA AIDA mission to a binary asteroid," COSPAR Sci. Assem., pp. 1–42, 2018, Accessed: Feb. 10, 2022. [Online]. Available: https://ui.adsabs.harvard.edu/abs/2018cosp...42E2280M/abstract.

[3] ESA Headquarters, "HERA Didymos reference model," 2021.

[4] ESA Estec, "HERA: Proximity Operations Guidelines," 2020.

[5] A. Pellacani, M. Graziano, M. Fittock, J. Gil, and I. Carnelli, "HERA vision based GNC and autonomy," Eur. Conf. Aerosp. Sci., pp. 1–14, 2019, doi: 10.13009/EUCASS2019-39.

[6] L. Pasqualetto Cassinis, A. Menicucci, E. Gill, I. Ahrns, and J. Gil-Fernández, "On-Ground Validation of a CNN-based Monocular Pose Estimation System for Uncooperative Spacecraft," 8th Eur. Conf. Sp. Debris, 2021.

[7] L. Pasqualetto Cassinis, R. Fonod, E. Gill, I. Ahrns, and J. Gil-Fernández, "Evaluation of tightly- and loosely-coupled approaches in CNN-based pose estimation systems for uncooperative spacecraft," Acta Astronaut., vol. 182, no. June 2020, pp. 189–202, 2021, [Online]. Available: https://doi.org/10.1016/j.actaastro.2021.01.035.

[8] K. Sun, B. Xiao, D. Liu, and J. Wang, "Deep high-resolution representation learning for human pose estimation," Proc. IEEE Comput. Soc. Conf. Comput. Vis. Pattern Recognit., vol. 2019-June, pp. 5686–5696, 2019, doi: 10.1109/CVPR.2019.00584.

[9] J. Gil-Fernandez and G. Ortega-Hernando, "Autonomous vision-based navigation for proximity operations around binary asteroids," CEAS Sp. J., vol. 10, no. 2, pp. 287–294, 2018, doi: 10.1007/s12567-018-0197-5.

[10] M. Pugliatti, V. Franzese, and F. Topputo, "Data-Driven Image Processing for Onboard Optical Navigation Around a Binary Asteroid," J. Spacecr. Rockets, pp. 1–17, 2022, doi: 10.2514/1.a35213.

[11] J. A. Christian, "Optical navigation using planet's centroid and apparent diameter in image," J. Guid. Control. Dyn., vol. 38, no. 2, pp. 192–204, 2015, doi: 10.2514/1.G000872.

[12] J. A. Christian and E. G. Lightsey, "Onboard image-processing algorithm for a spacecraft optical navigation sensor system," J. Spacecr. Rockets, vol. 49, no. 2, pp. 337–352, 2012, doi: 10.2514/1.A32065.

[13] NASA, "JPL Solar System Dynamics." https://ssd.jpl.nasa.gov/ (accessed Feb. 10, 2022).

[14] Dundee university, Planet and Asteroid Natural Scene Generation Utility User Manual, no. 4. 2019.

[15] ESA, "Hera Mission Instruments." https://www.heramission.space/hera-instruments (accessed Feb. 10, 2022).